Generation of Alfvén waves by high power pulse at the electron plasma frequency

B. Van Compernolle, W. Gekelman, P. Pribyl, and T. A. Carter

Department of Physics and Astronomy, University of California, Los Angeles, California, USA

Received 7 December 2004; revised 14 March 2005; accepted 21 March 2005; published 19 April 2005.

[1] The interaction of a short high power pulse at the electron plasma frequency (f = 9 GHz, τ = .5 μs, P < 70 kW) and a magnetized plasma ($n_0 \leq 1.25 \cdot 10^{12}$ cm^{-3}, B_0 = 1.0 – 2.5 kG, Helium) capable of supporting Alfvén waves has been studied. The interaction leads to the generation of inertial shear Alfvén waves. The Alfvén waves are centered in an azimuthal layer corresponding to the location of the plasma frequency cutoff. The Alfvén waves are monochromatic with frequency within 10% of the ion cyclotron frequency. Spatial patterns of the wave were measured at different axial and radial locations.
Citation: Van Compernolle, B., W. Gekelman, P. Pribyl, and T. A. Carter (2005), Generation of Alfvén waves by high power pulse at the electron plasma frequency, *Geophys. Res. Lett.*, *32*, L08101, doi:10.1029/2004GL022185.

1. Introduction

[2] The physics of the interaction between plasmas and high power waves at the electron plasma frequency is of importance in many areas of space and plasma physics. A great deal of laboratory research has been done on the interaction of microwaves in a density gradient when $\omega = \omega_{pe}$ in unmagnetized plasmas [*Stenzel et al.*, 1974; *Wong and Stenzel*, 1978; *Kim et al.*, 1974]. Extensive studies of HF-ionospheric modifications have been performed [*Fejer*, 1979] as evidenced by experiments at Arecibo [*Hansen et al.*, 1992; *Birkmayer et al.*, 1986; *Cheung et al.*, 1992; *Fejer et al.*, 1985], at the HAARP facility [*Rodriguez et al.*, 1998] in Alaska and at the EISCAT observatory in Norway [*Isham et al.*, 1999]. This paper focuses on the interaction with a fully magnetized plasma, capable of supporting Alfvén waves. The experiment is performed in the upgraded LArge Plasma Device (LAPD) at UCLA [*Gekelman et al.*, 1991] in a Helium plasma. A number of experiments have been done at LAPD using antennas, skin depth scale currents and laser produced plasmas to generate Alfvén waves [*Leneman et al.*, 1999; *Gekelman et al.*, 1997a, 1997b; *VanZeeland et al.*, 2001]. This Letter reports the production of Alfvén waves by a high power pulse at the electron plasma frequency. The absorption of these waves leads to a pulse of field aligned superthermal electrons. This electron current pulse then launches an Alfvén wave with $\omega \leq \omega_{ci}$. In space plasmas, there are many instances where pulses of field aligned superthermal electrons are observed. These pulses can be generated by various processes. In this experiment the microwave-plasma interaction is the means of generating the electron pulse. Superthermal electron pulses, with duration on the order of one ion gyroperiod, could generate Alfvén waves in space plasmas as well. The frequency spectrum of the Alfvén waves and the proposed generation mechanism also show strong similarities with electromagnetic ion-cyclotron waves observed in the aurora [*Temerin and Lysak*, 1984].

0094-8276/05/2004GL022185$05.00

2. Experimental Setup

[3] A schematic of the machine and a typical density profile are shown in Figure 1. The plasma is formed by a pulsed discharge ($I_d \approx 3.5$ kA) between cathode and mesh anode which are 55 cm apart. The discharge lasts for 10 ms, and is pulsed at 1 Hz. The plasma thus formed is highly reproducible. It is 18 m long, and has a diameter of 50 cm, which is more than a hundred ion larmor radii across at 1.0 kG. The background magnetic field was varied from 1.0 to 2.5 kG. The experiment was done in the afterglow (typically 2 ms after the termination of the discharge), so that the electron and ion populations are both cold ($T_e = T_i \approx .5$ eV). The microwave source generates .5 μs pulses with P $\simeq$ 70 kW at a frequency of 9 GHz. Near the horn, $|E_{microwaves}|^2/nT \gg 1$, where $E_{microwaves}$ denotes the electric field of the microwaves. The microwaves are guided through waveguides filled with SF_6 to prevent breakdown. They are then launched from a pyramidal horn antenna (11.4 cm by 9.1 cm aperture) through a side window of the machine. The polarisation of the horn was such that the electric field of the microwaves is parallel to the background magnetic field (O mode polarization).

[4] They propagate radially, across the background magnetic field, into the radial density gradient. The microwaves are plane waves by the time they reach the plasma edge (distance horn-plasma $\approx 10\ \lambda$). The peak density in the experiment was about $1.25 \cdot 10^{12}$ cm^{-3}. The 9 GHz microwave frequency corresponds to a critical density of 10^{12} cm^{-3}. This critical layer is typically 10 to 15 cm from the center of the machine. In these experiments $\omega_{pe,critical} > \omega_{ce}$ for all applied background magnetic fields.

[5] Measurements include microwave intensity measurements, low frequency (f $\leq$ 3 MHz) magnetic field measurements and flow measurements. The microwave intensity was measured using a three axis dipole probe, with the output signal rectified by a crystal diode. Low frequency magnetic field oscillations were measured with an inductive pickup probe consisting of three orthogonal coils. The coils were differentially wound to reduce electrostatic pickup. Density and flow measurements were done with a Mach probe [*Gunn et al.*, 2001]. Magnetic field data was acquired in several transverse planes (typically 40 cm by 40 cm) at different axial positions (.66, 1, 3 and 5 meters downstream

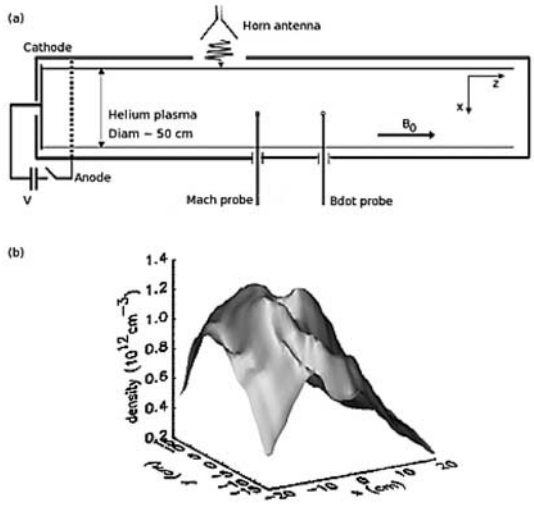

Figure 1. (a) Schematic of the experimental setup (not to scale). The plasma is formed by a pulsed discharge ($I_d \approx$ 3.5 kA) between anode and cathode which are 55 cm apart. The plasma has a duration of 10 ms, is reproducible and pulsed at 1 Hz. The B-dot probe and the Mach probe can be positioned at different axial and radial locations. (b) Typical density profile in a transverse plane 40 cm by 30 cm.

from the horn), and in several radial lines at those axial positions.

3. Experimental Results

[6] Data taken with the Mach probe (probe face size 1 mm^2, $V_{bias} = -45$ *V*, normal of the faces parallel to magnetic field) shows evidence of field aligned streaming electrons. Measurements were done in a transverse plane

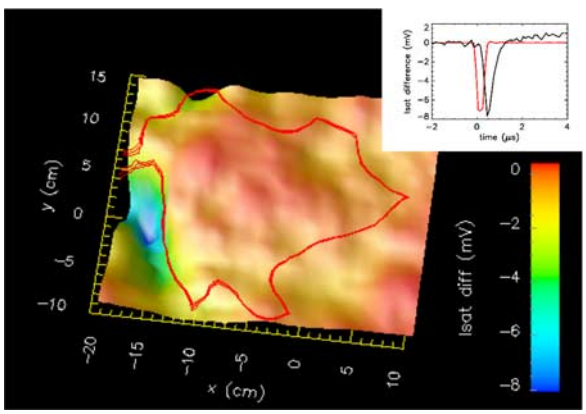

Figure 2. Transverse plane of the difference in ion saturation current between the two faces of the Mach probe. Shows the location of the streaming electrons in a plane 66 cm downstream from the location of microwave horn. The horn is located at x = −60 cm, y = 0 cm, z = 0 cm. Also plotted is the density contour corresponding to the critical density for the incoming microwaves (n = 10^{12} cm^{-3}). The insert shows a time trace (in black) at x = −20 cm, y = 2 cm. The streaming electrons are present for about 0.5 μs. The envelope of the microwave pulse is also shown (red curve).

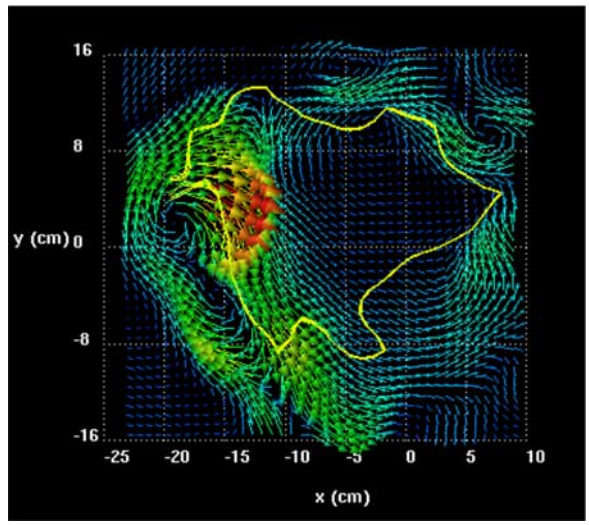

Figure 3. Vector plot of magnetic field of Alfvén wave in a xy plane at z = 3 m (B_0 = 2.0 kG). The horn is located at x = −60 cm, y = 0 cm, z = 0 cm. This plane was taken at t = 1.7 μs (t = 0 corresponds to the start of the microwave pulse). The yellow contour shows the critical density layer.

(40 cm by 30 cm, Δx = Δy = .8 cm) at z = 66 cm. The ion saturation current on the probe tip facing the interaction region shows a decrease .4 μs after the microwaves are launched, while the other probe tip does not. The decrease on the one face is due to electrons reaching the probe with energy greater than 45 eV. By taking the difference between the two faces we can subtract out the ion contribution to the current. The insert of Figure 2 shows a typical time trace. The peak is a signature of streaming electrons, with energy E > 45 eV. The fast electron peak lasts about .5 μs, which is on the same time scale as the microwave pulse length. Oscillations due to Alfvén waves are not picked up by the probe because it only collects the most energetic electrons, and because the waves are not strong enough to cause significant density perturbations. Figure 2 also shows a snapshot in time of the full data plane at the time of peak electron current. Also plotted is the density contour that corresponds to the critical density for the incoming microwaves. The strongest currents are observed just outside this contour, close to the location of the horn. The microwave intensity measurements, taken with the three axis dipole probe, are consistent with this figure. These intensity measurements showed that the highest microwave intensity occurs just outside the critical density contour, and on the side of the plasma closest to the horn. Apart from this, at other locations around the critical density contour we also detected microwaves, even on the other side of the plasma. This is due to multiple reflections of the microwaves between the critical cutoff layer and the stainless steel machine walls.

[7] Figure 3 shows a snapshot in time of the transverse magnetic field vectors in an xy plane at z = 3 m (B_0 = 2.0 kG). Overplotted is the density contour that corresponds to n = 10^{12} cm^{-3}, which is the location where the microwave frequency matches ω_{pe}. These magnetic field oscillations are observed in a layer about 15 cm wide, near the critical density contour. The strongest waves are excited

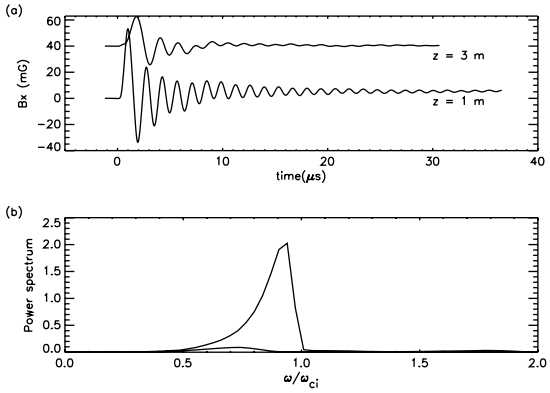

Figure 4. (a) Typical time traces of azimuthal magnetic field component at z = 1m and at z = 3 m. The trace at z = 3 m was offset by 40 mG. Both are 15 shot averages, with no frequency filtering. (b) Power spectrum of the time traces. Coherent peak (autocorrelation *e*-folding time ≈ 5 wave periods) near f_{ci} cut-off (f_{ci} = 760 kHz, B_0 = 2.0 kG) for the trace at z = 1 m. The frequency resolution is 24 kHz (≈3% of f_{ci}) because of the limited length of the time traces.

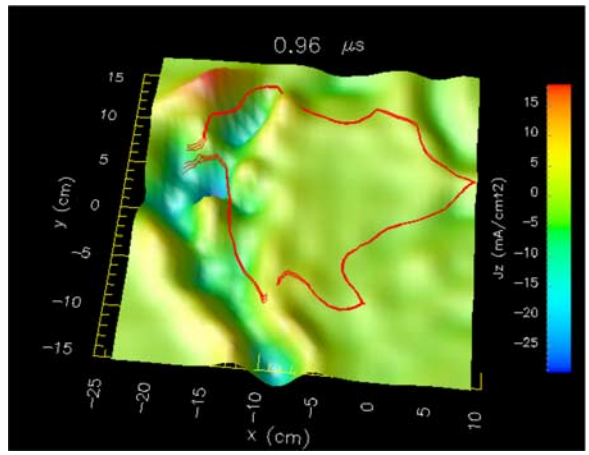

Figure 6. Snapshot in time of transverse plane of $j_z = \nabla \times B$ at t = .96 μs. Structure of outgoing currents, (colored blue-green) and return currents (colored red) can clearly be seen. Also shown is the contour corresponding to the critical density for the microwaves.

in the plasma on the side nearest the horn. Microwave reflections and scattering at the critical density contour and at the machine wall enable interactions around the entire column. On the left side of the plot the magnetic field vectors wrap around a region of a few cm wide and 10 cm long. This indicates that there is an axial current in that region. Note that the location of this current exactly corresponds to the location of the fast electrons in Figure 2. At a later time (t ≥ 3 μs) the field near the horn dominates the others. The oscillations at other places on the column are still there but are much smaller.

[8] A typical magnetic field component time trace, B_x, at z = 1 m is shown in Figure 4, along with its power spectrum. Field strengths are in the range of 20 mG ($\delta B/B_0 \simeq 10^{-5}$). These time traces are 15 shot averages, with no frequency filtering. The magnetic field was varied from 1.0 kG to 2.5 kG and all magnetic field oscillations exhibit similar spectra, when normalized to ω_{ci}. Further away, at z = 3 m and z = 5 m, the waves have lower frequencies, because the higher frequency modes are strongly damped. This is illustrated in the power spectra shown in Figure 4b. The transverse magnetic field components are generally a factor of 10 larger than the axial component. Varying the input power of the microwaves showed that the amplitude of these oscillations has a linear relationship with the input power of the microwaves. $B_{magn.osc.} \sim |E_{microwaves}|^2$, where $E_{microwaves}$ denotes the electric field of the microwaves.

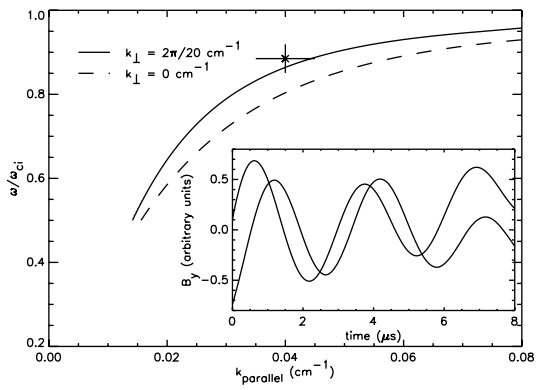

Figure 5. Theoretical dispersion relations for Alfvén waves with $k_\perp = 0$ cm^{-1}, $2\pi/20$ cm^{-1}. Measured dispersion matches curve for $k_\perp = 2\pi/20$ cm^{-1} within experimental error. Insert shows two time traces on same field line, but at different axial location (used to obtain $k_\parallel$).

[9] These magnetic oscillations are identified as shear Alfvén waves, after comparison with the theoretical dispersion relation. The frequency, parallel wave number and perpendicular wave number were measured. The perpendicular wave number is obtained by Fourier transforming the data in Figure 3 in space. The measurement was done with B_0 = 1.0 kG. This gave a value of .31 cm^{-1}, or $k_\perp = 2\pi/20$ cm^{-1}. The frequency was 340 kHz ± 13 kHz, therefore ω/ω_{ci} = .89 ± .034. The parallel wave number is obtained by examining the phase delay between time traces of a magnetic component of the wave, obtained on the same field line, but at different axial location (in this case at z = .67 m and at z = 1.0 m). These are plotted in the insert of Figure 5. The temporal difference between the phase maxima in the two traces is .62 ± .05 μs. Since $k_\parallel = \omega \cdot \Delta t/\Delta z$ with Δz = 33 cm, $k_\parallel$ = .040 ± .005 cm^{-1}. The lines plotted in Figure 5 correspond to the theoretically predicted dispersion relations for Alfvén waves. These curves were calculated by solving the dispersion relation [*Vincena et al.*, 2001]

$$n_\perp^2 n_\parallel^2 = \left(n_\parallel^2 - \epsilon_{xx}\right)\left(n_\perp^2 - \epsilon_\parallel\right) + \epsilon_{xy}^2\left(n_\perp^2 - \epsilon_\parallel\right)/\left(n^2 - \epsilon_{xx},\right) \quad (1)$$

for different values of $k_\perp$, and with T_e = .5 eV. In these equations, the plasma dispersion function Z was retained to include the effects of ion-cyclotron damping when $\omega \approx \omega_{ci}$. Also a Krook collision operator was introduced to include the effects of collisions. The measured magnetic oscillations lie indeed on the theoretical curve for $k_\perp = 2\pi/20$ cm^{-1},

within experimental error. This demonstrates that these are shear Alfvén waves, and since $v_{th,e} < v_A$ they are inertial shear Alfvén waves.

[10] The feature that separates these waves from Alfvén waves observed in previous experiments on LAPD [*Leneman et al.*, 1999; *Gekelman et al.*, 1997a, 1997b; *VanZeeland et al.*, 2001] is their frequency behavior. The time trace in Figure 4 looks like a single frequency damped oscillator. The power spectrum shows that the frequency of the wave is about 92% of the ion cyclotron frequency. The experiment was repeated with background magnetic fields, ranging from 1.0 kG to 2.5 kG, changing the ion cyclotron frequency by more than a factor of 2. The frequency of the Alfvén waves generated remained at $f \sim .92\, f_{ci}$ in all these experiments. Preliminary data of the experiment performed in an Argon plasma seems to indicate a similar behavior, with the observed Alfvén wave frequency even closer to the ion cyclotron frequency. As of yet, we do not have a full theoretical understanding as to why the Alfvén waves are monochromatic and are close to the ion cyclotron frequency.

[11] From the magnetic field measurements in a transverse plane we can derive the parallel wave current density along the axis, $j_z = \partial_x B_y - \partial_y B_x$. A snapshot in time is shown in Figure 6. Typical current densities are on the order of 30 mA/cm^2. The strongest currents occur in the region where the fast electrons were observed. These currents are surrounded on both sides by return currents, which are about half the size. The outgoing and return currents are the current system of the shear Alfvén wave. We believe that this current system is set up by the streaming electrons (Figure 2), generated during the microwave pulse. These streaming electrons in turn radiate the Alfvén wave. The initial electron current pulse generates an electromotive force, through Lenz's law, which forces background electrons to counterstream towards the interaction region, as to neutralize the local current imbalance. This sets up a system of field aligned outgoing and returning currents which excites Alfvén waves. The cross-field currents which close the current system are due to ion polarization drifts. The generation of Alfvén waves by axial electron currents has been observed in earlier experiments with laser produced plasmas and helical antennas [*VanZeeland et al.*, 2001; *Gekelman et al.*, 2000]. Electromagnetic ion-cyclotron waves in the aurora are also thought to be driven by field aligned electron currents [*Temerin and Lysak*, 1984].

4. Conclusions

[12] In summary, we have for the first time observed the generation of Alfvén waves by a process which initially involved waves in the electron plasma frequency range, four orders of magnitude higher in frequency. Due to reflections at the plasma edge and at the machine boundary, the microwaves irradiate the whole plasma column. The microwave-plasma interaction leads to the generation of a pulse of superthermal electrons, with $\Delta t \approx 2\pi/\omega_{ci}$, which then in turn launches an Alfvén wave. The waves have been identified as inertial shear Alfvén waves. Their frequency spectra peaks near the ion cyclotron frequency, irrespective of background magnetic field. Superthermal electron pulses, generated by other mechanisms, could also launch Alfvén waves in space plasmas. Further experiments will focus on the generation of fast electrons and the physics behind the frequency spectrum of the observed Alfvén waves.

[13] **Acknowledgments.** The authors wish to thank G. Morales, J. Maggs and S. Vincena for many useful discussions. This work was funded by the Department of Energy under award DE-FG03-98ER54494, and more recently by the National Science Foundation. The work was performed at the Basic Plasma Science User Facility at UCLA, which is funded by NSF/DOE.

References

Birkmayer, W., T. Hagfors, and W. Kofman (1986), Small-scale plasma-density depletions in Arecibo high-frequency modification experiments, *Phys. Rev. Lett.*, *57*, 1008.

Cheung, P. Y., D. F. Dubois, T. Fukuchi, K. Kawan, H. A. Rose, D. Russel, T. Tanikawa, and A. Y. Wong (1992), Investigation of strong Langmuir turbulence in ionospheric modification, *J. Geophys. Res.*, *97*, 10,575.

Fejer, J. A. (1979), Ionospheric modification and parametric instabilities, *Rev. Geophys.*, *17*, 135.

Fejer, J. A., C. A. Gonzales, H. M. Ierkic, M. P. Sulzer, C. A. Tepley, L. M. Duncan, F. T. Djuth, S. Ganguly, and W. E. Gordon (1985), Ionospheric modification experiments with the Arecibo heating facility, *J. Atmos. Terr. Phys.*, *47*, 1165.

Gekelman, W., H. Pfister, Z. Lucky, J. Bamber, D. Leneman, and J. Maggs (1991), Design, construction, and properties of the large plasma research device—The LAPD at UCLA, *Rev. Sci. Instrum.*, *62*, 2875.

Gekelman, W., S. Vincena, D. Leneman, and J. Maggs (1997a), Experimental observations of shear Alfvén waves generated by narrow current channels, *Plasma Phys. Controlled Fusion*, *39*, A101.

Gekelman, W., S. Vincena, D. Leneman, and J. Maggs (1997b), Laboratory experiments on shear Alfvén waves and their relationship to space plasmas, *J. Geophys. Res.*, *102*, 7225.

Gekelman, W., S. Vincena, N. Palmer, P. Pribyl, D. Leneman, C. Mitchell, and J. Maggs (2000), Experimental measurements of the propagation of large amplitude shear Alfvén waves, *Plasma Phys. Controlled Fusion*, *42*, B15.

Gunn, J. P., et al. (2001), Edge flow measurements with Gundestrup probes, *Phys. Plasmas*, *8*, 1995.

Hansen, J. D., G. J. Morales, L. M. Duncan, and G. Dimonte (1992), Large-scale HF-induced ionospheric modifications: Experiments, *J. Geophys. Res.*, *97*, 113.

Isham, B., C. L. Hoz, M. T. Rietveld, T. Hagfors, and T. B. Leyser (1999), Cavitating Langmuir turbulence observed during high-latitude ionospheric wave interaction experiments, *Phys. Rev. Lett.*, *83*, 2576.

Kim, H. C., R. L. Stenzel, and A. Y. Wong (1974), Development of cavitons and trapping of RF field, *Phys. Rev. Lett.*, *33*, 886.

Leneman, D., W. Gekelman, and J. Maggs (1999), Laboratory observations of shear Alfvén waves launched from a small source, *Phys. Rev. Lett.*, *82*, 2673.

Rodriguez, P., et al. (1998), The WIND-HAARP experiment: Initial results of high power radiowave interactions with space plasmas, *Geophys. Res. Lett.*, *25*, 257.

Stenzel, R. L., A. Y. Wong, and H. C. Kim (1974), Conversion of electromagnetic waves to electrostatic waves in inhomogeneous plasmas, *Phys. Rev. Lett.*, *32*, 654.

Temerin, M., and R. L. Lysak (1984), Electromagnetic ion cyclotron mode (ELF) waves generated by auroral electron precipitation, *J. Geophys. Res.*, *89*, 2849.

VanZeeland, M., W. Gekelman, S. Vincena, and G. Dimonte (2001), Production of Alfvén waves by a rapidly expanding dense plasma, *Phys. Rev. Lett.*, *87*, doi:10.1103/PhysRevLett.87.105001.

Vincena, S., W. Gekelman, and J. Maggs (2001), Shear Alfvén waves in a magnetic beach and the roles of electron and ion damping, *Phys. Plasmas*, *8*, 3884.

Wong, A. Y., and R. L. Stenzel (1978), Ion acceleration in strong electromagnetic interactions with plasmas, *Phys. Rev. Lett.*, *34*, 727.

T. A. Carter, W. Gekelman, P. Pribyl, and B. Van Compernolle, Department of Physics and Astronomy, University of California, 1000 Veteran Ave., Rm. 15-70, Los Angeles, CA 90095–1547, USA. (bvcomper@physics.ucla.edu)